

## OPEN ACCESS

## EDITED BY

Frédéric Frézard,  
Federal University of Minas Gerais, Brazil

## REVIEWED BY

Zhen Zhao,  
University of Southern California,  
United States  
Mark Endsley,  
University of Texas Medical Branch at  
Galveston, United States

## \*CORRESPONDENCE

Cordelia Dunai  
✉ cdunai@liverpool.ac.uk  
Benedict D. Michael  
✉ benmic@liverpool.ac.uk

## †PRESENT ADDRESSES

Jordan J. Clark,  
Department of Microbiology, Icahn School of  
Medicine at Mount Sinai, New York, New  
York, NY, United States;  
Center for Vaccine Research and Pandemic  
Preparedness, Icahn School of Medicine at  
Mount Sinai, New York, NY, United States  
Sarosh R. Irani,  
Department of Neurology, Mayo Clinic  
Florida, Jacksonville, FL, United States;  
Department of Neurosciences, Mayo Clinic  
Florida, Jacksonville, FL, United States  
Robyn Williams,  
Department of Neurology, Mayo Clinic  
Florida, Jacksonville, FL, United States;  
Department of Neurosciences, Mayo Clinic  
Florida, Jacksonville, FL, United States

†These authors have contributed equally to  
this work

RECEIVED 29 May 2024

ACCEPTED 04 September 2024

PUBLISHED 14 October 2024

## CITATION

Dunai C, Hetherington C, Boardman SA,  
Clark JJ, Sharma P, Subramaniam K,  
Tharmaratnam K, Needham EJ, Williams R,  
Huang Y, Wood GK, Collie C, Fower A, Fox H,  
Ellul MA, Held M, Egbe FN, Griffiths M,  
Solomon T, Breen G, Kipar A, Cavanagh J,  
Irani SR, Vincent A, Stewart JP, Taams LS,  
Menon DK and Michael BD (2024) Pulmonary  
SARS-CoV-2 infection leads to para-  
infectious immune activation in the brain.  
*Front. Immunol.* 15:1440324.  
doi: 10.3389/fimmu.2024.1440324

# Pulmonary SARS-CoV-2 infection leads to para-infectious immune activation in the brain

Cordelia Dunai<sup>1,2\*</sup>, Claire Hetherington<sup>2</sup>, Sarah A. Boardman<sup>2</sup>,  
Jordan J. Clark<sup>3†</sup>, Parul Sharma<sup>3</sup>, Krishanthi Subramaniam<sup>3</sup>,  
Kukatharmini Tharmaratnam<sup>4</sup>, Edward J. Needham<sup>5</sup>,  
Robyn Williams<sup>6†</sup>, Yun Huang<sup>2</sup>, Greta K. Wood<sup>2</sup>, Ceryce Collie<sup>2</sup>,  
Andrew Fower<sup>6</sup>, Hannah Fox<sup>6</sup>, Mark A. Ellul<sup>2</sup>, Marie Held<sup>7</sup>,  
Franklyn N. Egbe<sup>2</sup>, Michael Griffiths<sup>2</sup>, Tom Solomon<sup>1,2,8</sup>,  
Gerome Breen<sup>9,10</sup>, Anja Kipar<sup>3,11</sup>, Jonathan Cavanagh<sup>12</sup>,  
Sarosh R. Irani<sup>8†</sup>, Angela Vincent<sup>6</sup>, James P. Stewart<sup>3</sup>,  
Leonie S. Taams<sup>13†</sup>, David K. Menon<sup>14‡</sup>  
and Benedict D. Michael<sup>1,2,8\*†</sup>

<sup>1</sup>NIHR Health Protection Research Unit in Emerging and Zoonotic Infections, Liverpool, United Kingdom,

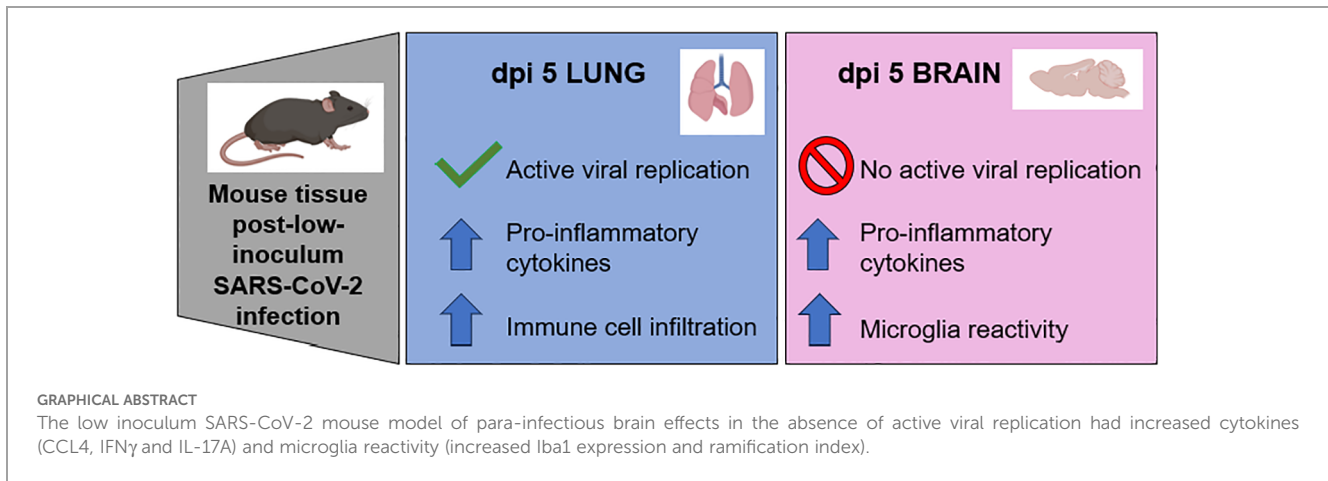
<sup>2</sup>Clinical Infection Microbiology and Immunology, Institute of Infection Ecology and Veterinary Sciences, University of Liverpool, Liverpool, United Kingdom, <sup>3</sup>Department of Infection Biology and Microbiomes, Institute of Infection, Veterinary and Ecological Sciences, University of Liverpool, Liverpool, United Kingdom,

<sup>4</sup>Department of Health Data Science, Institute of Population Health, Faculty of Health and Life Sciences, University of Liverpool, Liverpool, United Kingdom, <sup>5</sup>Department of Clinical Neurosciences, University of Cambridge, Cambridge, United Kingdom, <sup>6</sup>Nuffield Department of Clinical Neurosciences, Medical Sciences Division, University of Oxford, Oxford, United Kingdom, <sup>7</sup>Centre for Cell Imaging, Faculty of Health and Life Sciences, University of Liverpool, Liverpool, United Kingdom, <sup>8</sup>Department of Neurology, The Walton Centre NHS Foundation Trust, Liverpool, United Kingdom, <sup>9</sup>Department of Social, Genetic & Developmental Psychiatry Centre, School of Mental Health & Psychological Sciences, King's College London, London, United Kingdom, <sup>10</sup>NIHR Maudsley Biomedical Research Centre, King's College London, London, United Kingdom, <sup>11</sup>Laboratory for Animal Model Pathology, Institute of Veterinary Pathology, Vetsuisse Faculty, University of Zurich, Zurich, Switzerland, <sup>12</sup>College of Medical, Veterinary and Life Sciences, University of Glasgow, Glasgow, United Kingdom, <sup>13</sup>Centre for Inflammation Biology and Cancer Immunology, Department of Inflammation Biology, School of Immunology & Microbial Sciences, Faculty of Life Sciences & Medicine, King's College London, London, United Kingdom, <sup>14</sup>Division of Anaesthesia, Addenbrooke's Hospital, Cambridge University Hospitals, Cambridge, United Kingdom

Neurological complications, including encephalopathy and stroke, occur in a significant proportion of COVID-19 cases but viral protein is seldom detected in the brain parenchyma. To model this situation, we developed a novel low-inoculum K18-hACE2 mouse model of SARS-CoV-2 infection during which active viral replication was consistently seen in mouse lungs but not in the brain. We found that several mediators previously associated with encephalopathy in clinical samples were upregulated in the lung, including CCL2, and IL-6. In addition, several inflammatory mediators, including CCL4, IFN $\gamma$ , IL-17A, were upregulated in the brain, associated with microglial reactivity. Parallel *in vitro* experiments demonstrated that the filtered supernatant from SARS-CoV-2 virion exposed brain endothelial cells induced activation of uninfected microglia. This model successfully recreates SARS-CoV-2 virus-associated para-infectious brain inflammation which can be used to study the pathophysiology of the neurological complications and the identification of potential immune targets for treatment.

## KEYWORDS

virology, immunology, SARS-CoV-2, neurology, microglia



## Introduction

SARS-CoV-2 infection has been associated with a range of neurological complications. Although their incidence has decreased with widespread vaccination and effective anti-viral and anti-inflammatory treatments, they remain a significant clinical issue (1). A large retrospective study with contemporary controls found neurological complications were more common in people who had experienced COVID-19 but were also found in non-hospitalised/mild cases of COVID-19, revealing a large healthcare burden left in the wake of the pandemic (2). The different neurological complications, ranging from loss of smell to encephalitis, caused by SARS-CoV-2 infection most likely have very different aetiologies, but viral protein is seldom found in the brain parenchyma strongly suggesting that indirect effects of the virus, such as immune-mediated pathologies, are a likely potential cause (3–6). Indeed, we and others previously found that COVID-19 patients with neurological complications had elevated serum immune mediators and cytokines (IL-6, IL-12p40, IL1-RA, M-CSF, CCL2, and HGF) which correlated with serum brain injury markers (7–10).

Mouse models are important to systematically study early changes in disease and disease progression, but most models of SARS-CoV-2 have involved systemic dissemination with brain pathology that may not reflect the clinical scenarios (11–14). We established a mouse model using an inoculum of virus ten times lower than that which earlier studies have used, and looked for evidence of brain immune activation in the absence of viral replication in the brain. We also developed an *in vitro* assay to investigate how exposure of endothelial cells to viral protein can lead to cytokine-mediated indirect effects on microglia, which we hypothesize is the most common clinical scenario for how SARS-CoV-2 affects the brain (15).

## Methods

### Mouse studies of infection with SARS-CoV-2

An AWERB-approved protocol was followed for the mouse studies (University of Liverpool Animal Welfare and Ethical Review

Body, UK Home Office Project Licence PP4715265). Mice were maintained under SPF barrier conditions in individually ventilated cages. Male and female 2–4 month old heterozygote hACE2-transgenic C57BL/6 mice (Charles River Laboratory) were infected intranasally with  $1 \times 10^3$  or  $1 \times 10^4$  plaque-forming units (PFU) of a human isolate of SARS-CoV-2 (Pango B lineage hCoV-2/human/Liverpool/REMRQ0001/2020) under isoflurane anaesthesia. Mice were euthanized on day 5 post infection. Brains were perfused with 30mL PBS w/1mM EDTA, then one hemisphere fixed in formaldehyde-containing PLP buffer overnight at 4°C. Brains were then subjected to a sucrose gradient– 10 and 20% sucrose for 1hr each and then 30% sucrose O/N at 4°C. Brains were then frozen in OCT by submerging moulds in a beaker of 2-methylbutane on dry ice. The other hemisphere was divided in two sagittal sections and half preserved in 4%PFA for histology and half in trizol for RNA and protein extraction. Sera was collected and frozen and then heat-inactivated at 56°C for 30 mins prior to be moved from CL3 to CL2 lab. Lung tissue was preserved in 4%PFA for histology, in trizol for RNA and protein extraction, and in PLP for cryosectioning. Cytokines were measured from tissue protein extract with Bio-rad reagents on a Bio-plex 200 following the manufacturer's protocol.

### qPCR of SARS-CoV-2 genes and mouse cytokines

Gene expression was measured from trizol isolated RNA (Invitrogen cat# 15596018, manufacturer's protocol) using Promega's GoTaq Probe 1-Step RT-qPCR system (cat#A6120, manufacturer's protocol) on an Agilent AriaMx. Primers and FAM probes for SARS-CoV-2, cytokines, and housekeeping genes were purchased from IDT (Tables 1, 2) with standard IDT qPCR primer/probe sets for the mouse cytokines.

The thermal cycle for N1 and the mouse cytokines was: 45°C for 15min 1x, 95°C for 2 min, then 45 cycles of 95°C for 3 secs followed by 55°C for 30 sec.

For subgenomic E: 45°C for 15 min 1x, 95°C for 2 min, then 45 cycles of 95°C for 15 secs followed by 58°C for 30 sec.

TABLE 1 Primers and probes for viral genes and normalization.

Gene	Reagent	IDT Cat#	Sequence (5'–3')
N1	Forward primer:	10006830	GACCCCAAAATCAGCGAAAT
	Reverse primer:	10006831	TCTGGTACTGCCAGTTGAATCTG
	FAM probe:	10006832	ACCCCGCATTACGTTTGGTGGACC
subgE	Forward primer:	10006889	CGATCTCTGTAGATCTGTTCTC
	Reverse primer:	10006891	ATATTGCAGCAGTACGCACACA
	FAM probe:	10006893	ACACTAGCCATCCTTACTGCGCTTCG
18S	Forward primer:	Custom	ACCTGGTTGATCCTGCCAGTAG
	Reverse primer:	Custom	AGCCATTTCGAGTTTCACTGTAC
	FAM probe:	Custom	TCAAAGATTAAGCCATGCATGTCTAAGTACGCAC

For 18S it was: 45°C for 15 min, 95°C for 2 min and 40 cycles of 95°C for 15s, 60°C for 1 min.

## Histology and confocal microscopy

Paraffin-embedded formalin-fixed tissue was sectioned to 4 μm sections. Slides were baked at 60°C for 30 minutes and then stained with H&E in an autostainer. H&E slides were imaged on a Leica microscope. For immunofluorescent staining and confocal microscopy, OCT-embedded frozen tissue was sectioned to 12 μm or 30 μm sections (thicker sections needed for the Z-stack imaging and microglia ramification/reactivation quantification). 100% acetone was used for antigen retrieval (10 mins at room temperature). After air-drying, then PBS washing, tissue sections were permeabilized with 0.1% Triton X-100/PBS (20 mins at room temperature). After rinsing with PBS, tissue sections were blocked with Dako block (5 minutes at room temperature). After another PBS wash, primary antibodies were added at dilutions listed in table for an overnight incubation at 4°C in a humidified chamber. Tissue sections were washed twice with PBS for 5 minutes each wash. Secondary antibody (as described in Table 3) was added for a 2 hr room

temperature incubation, followed by two 5-minute PBS washes. DAPI-mounting medium was used for coverslipping. Imaging was performed with Andor Dragonfly spinning disk confocal microscope. Marker fluorescence and microglia counts, intensity, and reactivation indices [method based on previous work (16, 17)] were quantified with Fiji (confocal microscope set up in Table 4 and macros downloadable from the public [Github repository](#)). The reactivation index is the area of the cell divided by the projection area (the whole polygon covered by the cell). Reactivation indices of 0-1 of objects with a threshold size of 19 μm<sup>2</sup> were quantified from three Z-stack images/mouse and two mice/group.

## In vitro cell culture assays

The investigated cell lines were cultured according to the manufacturer's recommendations. The mouse brain endothelial cell line, bEnd.3 (ECACC 96091929) was used between passage 22 and 29. The cells were cultured in Dulbecco's Modified Eagle Medium (DMEM) supplemented with 2mM Glutamine, 5μM 2-Mercaptoethanol (2ME), 1mM Sodium Pyruvate (NaP), 1% Non Essential Amino Acids (NEAA), 10% Foetal Bovine Serum (FBS) and 1X penicillin/streptomycin (P/S). Primary mouse microglia (ScienCell, SC-M1900-57) were cultured on poly-L-lysine (ScienCell 0413) coated flasks in Microglia medium (ScienCell 1901) supplemented with 1% FBS, 1x microglia growth supplement (MGS, ScienCell 1952) and 1 x P/S. Primary mouse astrocytes were cultured on poly-L-lysine (ScienCell 0413) coated flasks in Astrocyte Medium (ScienCell 1801) supplemented with 2% FBS, 1x astrocyte growth supplement (AGS, ScienCell 1852) and 1 x P/S.

## In vitro incubation with inactivated virus and endothelial supernatants

Acid/heat inactivated SARS-CoV-2 (B.1.1.7) (NIBSC 101027) of known titre was used for all experiments. For incubation with inactivated virus, cells were seeded into either 24 well plates or 6 well plates at 125,000 cells per cm<sup>2</sup> and allowed to adhere overnight. Virus dilutions were then prepared to give a ratio of 1 copy (MOI 1),

TABLE 2 Primers and probes for mouse cytokines.

Gene	IDT Primetime Cat#
IL-1RN	Mm.PT.58.43781580
IL-6	Mm.PT.58.10005566
IL-12p40	Mm.PT.58.12409997
M-CSF	Mm.PT.58.11661276
CCL2	Mm.PT.58.42151692
HGF	Mm.PT.58.9088506
CCL4	Mm.PT.58.5219433
IFNG	Mm.PT.58.41769240
IL-17A	Mm.PT.58.6531092

For mouse cytokines, the primer/probe sets listed in Table 2 were used and the cycle was: 45°C for 15 min; 95°C for 2 min; 45 cycles of 95°C for 3 sec and 55°C for 30 sec.

TABLE 3 Antibodies for immunofluorescent stain and confocal imaging.

Antibody target-fluorochrome	Company	Cat#	Host	Dilution Factor (for 200 $\mu$ L per section)
CD45-PE	Invitrogen	12-0451-82	Rat	50
CD11b-AF647	BDBioscience	557686	Rat	200
NK1.1-AF488	BioLegend	108718	Mouse	100
CD3-FITC	Abcam	ab34722	Rat	50
GFAP	Invitrogen	41-9892-82	Mouse	100
NeuN	Merck	MAB377X	Mouse	100
CD68 unconjugated	Abcam	ab53444	Rat	200
Anti-rat AF488	Jackson ImmunoResearch	712-546-153	Donkey	500
Iba1 unconjugated	Wako	019-19741	Rabbit	500
Anti-rabbit IgG-AF647	Invitrogen	A-31573	Donkey	500
Spike unconjugated	Invitrogen	703958	Human	100
Anti-human AF568	Fisher	A-21090	Goat	500

0.1 copies (MOI 0.1) or 0.01 copies (MOI 0.01) per cells plated in the culture medium. For bEnd.3 experiments, cells were incubated for 24 hours with inactivated virus, 20  $\mu$ g/mL polyI:C (Merck PL530) or with untreated culture medium. For astrocyte and microglia experiments, cells were incubated for 2 hours with inactivated virus, polyI:C, untreated medium, or supernatant from bEnd.3 cells previously exposed for 24 hours to MOI 1 virus dilution. Supernatant from bEnd.3 cells was filtered with a 20 nm syringe filter directly prior to treating microglia and astrocytes to remove viral particles. After 2 hours, treatments were removed, cells were washed with 1X phosphate-buffered saline (PBS) (Capricorn Scientific CSR154) three times and then the normal culture medium was replaced. For each treatment condition (virus or supernatant) 6-7 individual well replicates were performed and for control conditions (polyI:C or untreated) 3-4 replicates were performed. After 24 hours, the supernatant from these cells was collected and cells were fixed with 4% paraformaldehyde (Sigma 16005).

## ELISA of *in vitro* supernatants

Supernatants were collected into 1 mL cryovials and stored at 4°C for no longer than 1 week prior to cytokine levels being assessed using ELISA. Kits were purchased from Invitrogen for IL-6 (88-7064), CCL2 (88-7391), IFN $\gamma$  (88-7314) and performed according to manufacturer's protocol.

## Immunostaining of *in vitro* samples

Microglia were fixed with 4% paraformaldehyde and washed 3x with 1X PBS with calcium and magnesium (PBS +/+) (Capricorn Scientific CSR1576). Cells were then incubated for 1 hour with Dakoblock (Agilent X090930-2). Cells were then washed 1x with PBS and incubated with primary antibody (Iba1 Wako Chemicals 019-19741; CD45-PE Thermo Fisher 12-0451-83) diluted in

antibody diluent (1X PBS +/+, 1% BSA, 10% donkey serum (Sigma D9663), 0.1% Triton-X (Sigma X100)) overnight at 4°C. Cells were then washed 3x with 1x PBS +/+ and incubated with secondary antibody (Donkey anti-rabbit AF657, Thermo Fisher A31573) and DAPI (Thermofisher P36962) in antibody diluent and incubated in the dark for 2 hours at room temperature. Cells were then washed 3x with PBS +/+.

TABLE 4 Confocal microscopy settings.

Microscope component	Parameters
Microscope	Leica DMI8 with Andor Dragonfly
Light source	7-line integrated laser engine equipped with: Solid state 405 smart diode laser at 100mW: set to 10% Solid state 488 smart diode laser at 50mW: set to 35% OBIS LS 561 smart OPSS laser at 50mW: set to 2.0% OBIS LX Solid state 637 smart diode laser at 140mW: set to 7.0%
Excitation/emission optics	Dichroic mirror: Quad EM filter 405-488-561-640 Dual camera beam splitter: Dual camera dichroic 565nm long pass Emission filters: 450/50nm bandpass filter 525/50nm bandpass filter 600/50nm bandpass filter 700/75nm bandpass filter Spinning disk with 40 $\mu$ m pinholes
Objective lenses	Leica objectives: 11506358 HC PL APO 40x/1.30 OIL CS2
Detector	Andor iXon Ultra 888 Ultra EMCCD Camera 1024 $\times$ 1024; 405: 500 ms exposure; 65 EM gain 488: 500 ms exposure; 65 EM gain 561: 30 ms exposure; 156 EM gain 637: 30 ms exposure; 156 EM gain Averaging: 1; Binning: 1; camera magnification 1x Nyquist Z sampling

## In vitro confocal microscopy and reactivation/ramification index quantitation

Microglia were imaged at 25x magnification on a Leica DMI8 on an Andor Dragonfly spinning disk confocal microscope. 16 images per well were taken and stitched into a tilescan image using Fusion imaging software. Tilescan images were then processed in Fiji/ImageJ by thresholding the PE/647 channel and gating for individual cells (excluding cell clusters) and then analysing particles between 500-1000  $\mu\text{m}$  for solidity.

## Statistical analyses

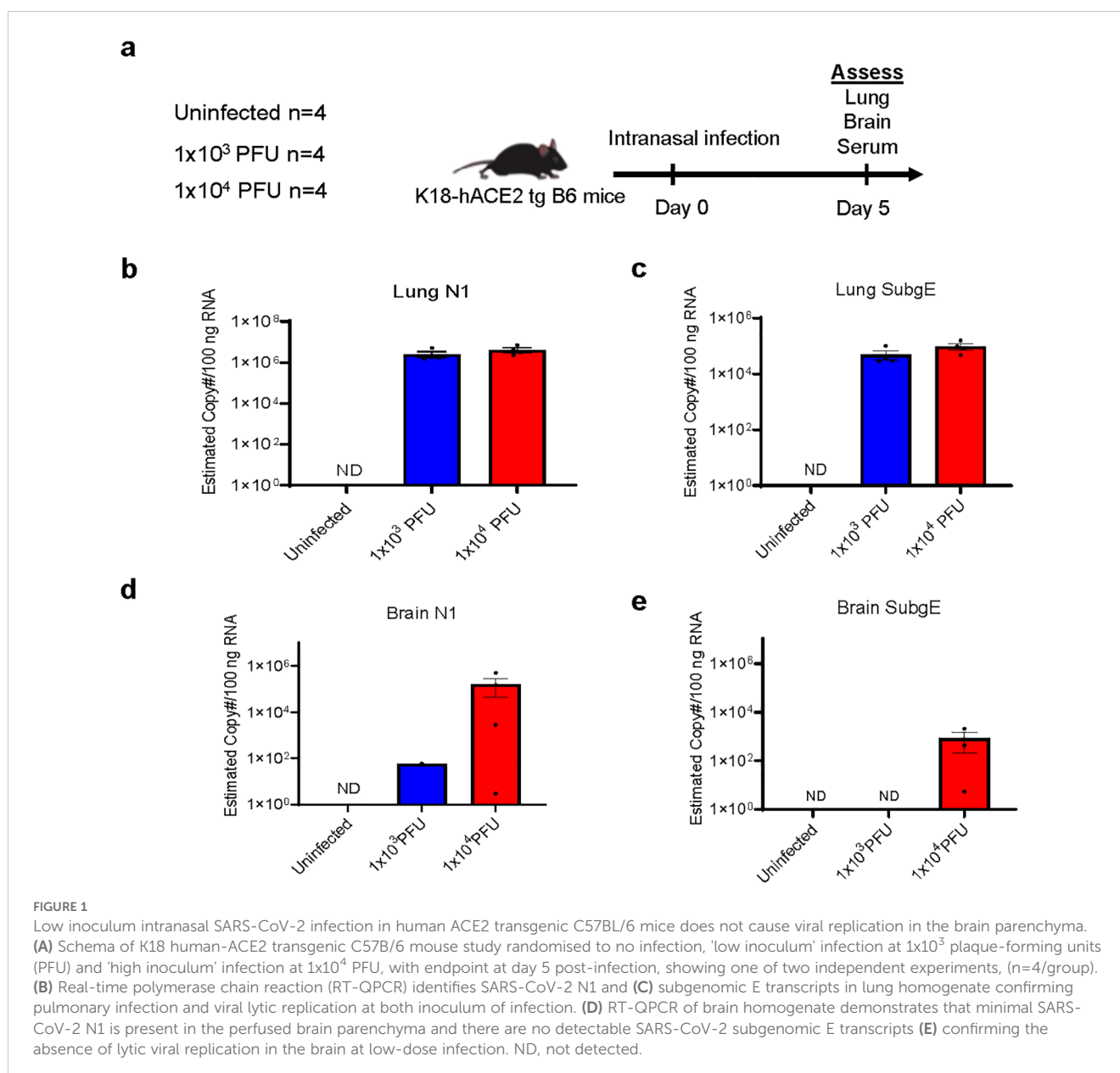
Prism software (version 9.4.1, GraphPad Software Inc.) was used for graph generation and statistical analysis. The Shapiro-Wilk normality test used to check the normality of the distribution. Data

are expressed as mean  $\pm$  S.E.M. The difference between two or more non-normally distributed groups was tested using Mann-Whitney U or Kruskal-Wallis tests, respectively.  $P \leq 0.05$  was considered statistically significant.

## Results

### Low inoculum intranasal SARS-CoV-2 infection in human ACE2 transgenic C57BL/6 mice does not cause viral replication in the brain parenchyma

We established the mouse model by comparing intranasal infection with a low ( $1 \times 10^3$  PFU) and a high ( $1 \times 10^4$  PFU) inoculum of SARS-CoV-2, collecting serum, brain and lung tissues at day 5 post-infection (Figure 1A). At this stage, none



of the mice showed weight loss (Supplementary Figure 1A). Both levels of infection caused pathology in the lung, with viral loads evidenced by qPCR of N1 with both low and high inocula (Figure 1B). There was also evidence of active viral replication in the lung, as defined by the surrogate readout of qPCR of subgenomic E which correlates with infectivity (18) (Figure 1C). SARS-CoV-2 N1 transcripts were detected in four out of four brains of mice that had received high inoculum of SARS-CoV-2 and in six of nine that received low inoculum (Figure 1D; first experiment displayed, n=4 group). However, whilst three of four high inoculum mice showed active viral transcription in the brain by the detection of subgenomic E, this was only detectable in two of nine low inoculum mouse brains (tissue from these two animals were not included in subsequent ex vivo experiments, Figure 1E; Supplementary Figures 1E–G).

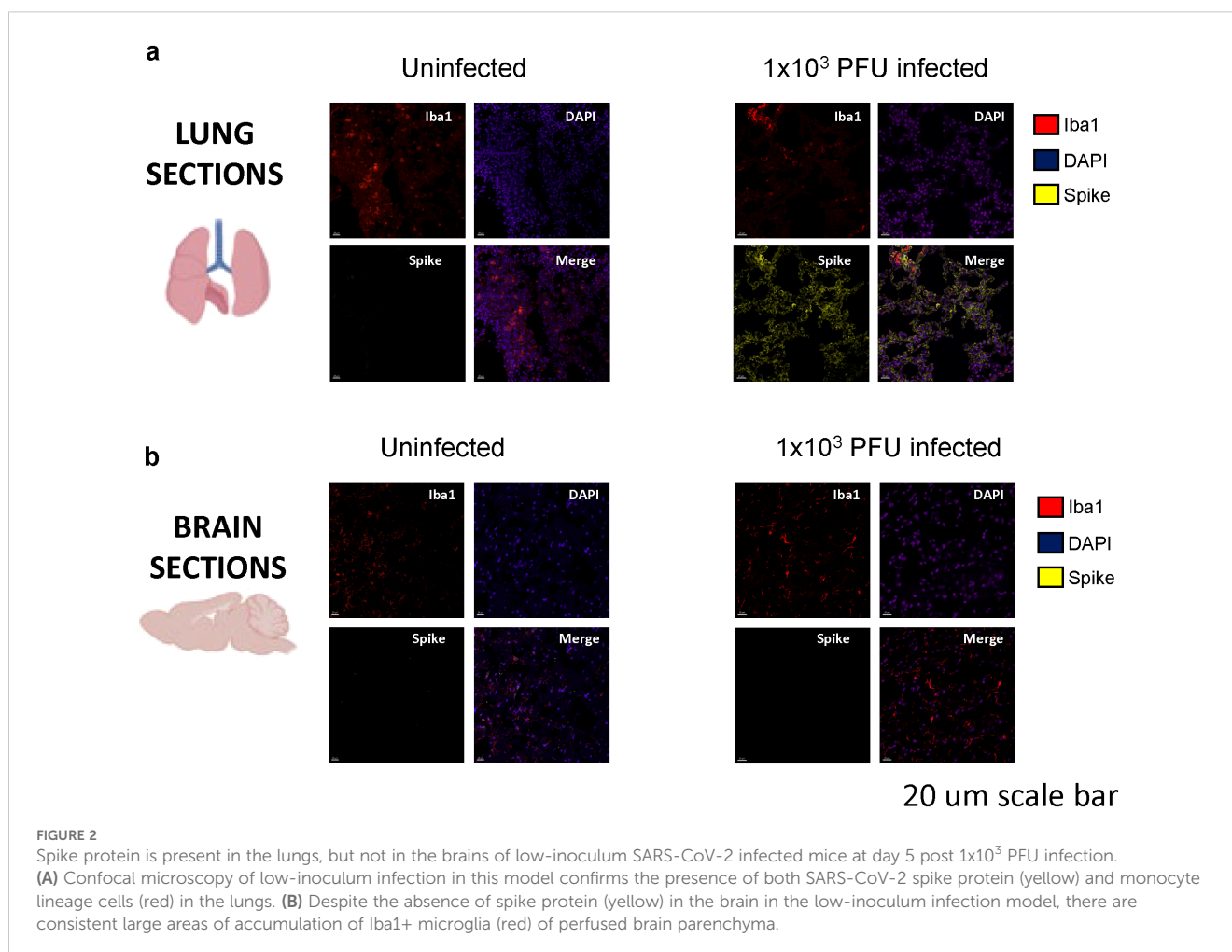
H&E staining of lung and brain sections from infected mice were assessed for pathology and mononuclear cell clusters (Supplementary Figures 1B–D). The lungs of SARS-CoV-2 infected mice showed signs of pathology including oedema, haemorrhage, and fibrosis (Supplementary Figure 1B). Mononuclear cells were present with both inocula compared with uninfected mice (Supplementary Figure 1B). The brain tissue also had a few clusters of mononuclear cells in the frontal cortex with both inocula of SARS-CoV-2 (Supplementary Figures 1C, D).

## Spike protein is present in the lungs, but not brains, of $1 \times 10^3$ PFU SARS-CoV-2 infected mice and there are differences in immune activation

Immunofluorescent staining and confocal microscopy of the lungs showed large amounts of viral spike protein with increased Iba1 expression (Figure 2A). The lungs also showed increases in CD45 and CD11b staining compared with uninfected animals (Figure 3A). Confocal microscopy of ex vivo brain sections from mice, following the low inoculum, demonstrated Iba-1 staining but, in contrast to lung tissue, showed no evidence of staining for SARS-CoV-2 spike protein (Figures 2B, 3B). These brains also showed no increases in numbers of CD3+ or NK1.1+ cells (Supplementary Figures 2A, B), or apoptotic cells (Supplementary Figure 2C).

## Several inflammatory mediators are elevated in the lungs and brains of $1 \times 10^3$ PFU SARS-CoV-2 infected mice

In order to understand the mechanisms driving this apparent para-infectious neuropathology, we assessed transcription and protein levels of inflammatory mediators in brains and lung from the seven



low-inoculum infected mice that showed no evidence of local viral replication in the brain. Our previous clinical study, comparing serum immune mediators from low vs. normal Glasgow coma scale score COVID-19 patients, demonstrated that six mediators of interest were increased in serum (7). Lung tissue from the mice revealed four of these, IL1-RA, IL-6, CCL2, and IL-12p40, to be upregulated with low-inoculum infection by QPCR (Figures 4A, B).

The brains from low inoculum infected mice showed increased transcripts of CCL4 and decreased levels of IL-1RA and IL-12p40 (Figures 4C, D; Supplementary Table 1). Although many brain cytokine proteins were not different between uninfected and low inoculum mice, CCL4, IFN $\gamma$  and IL-17A were increased (Figures 4E, F; Supplementary Table 2). Consistent with an intra-cerebral local response, there were no increases in any of these cytokines in the mouse sera (Figures 4G, H).

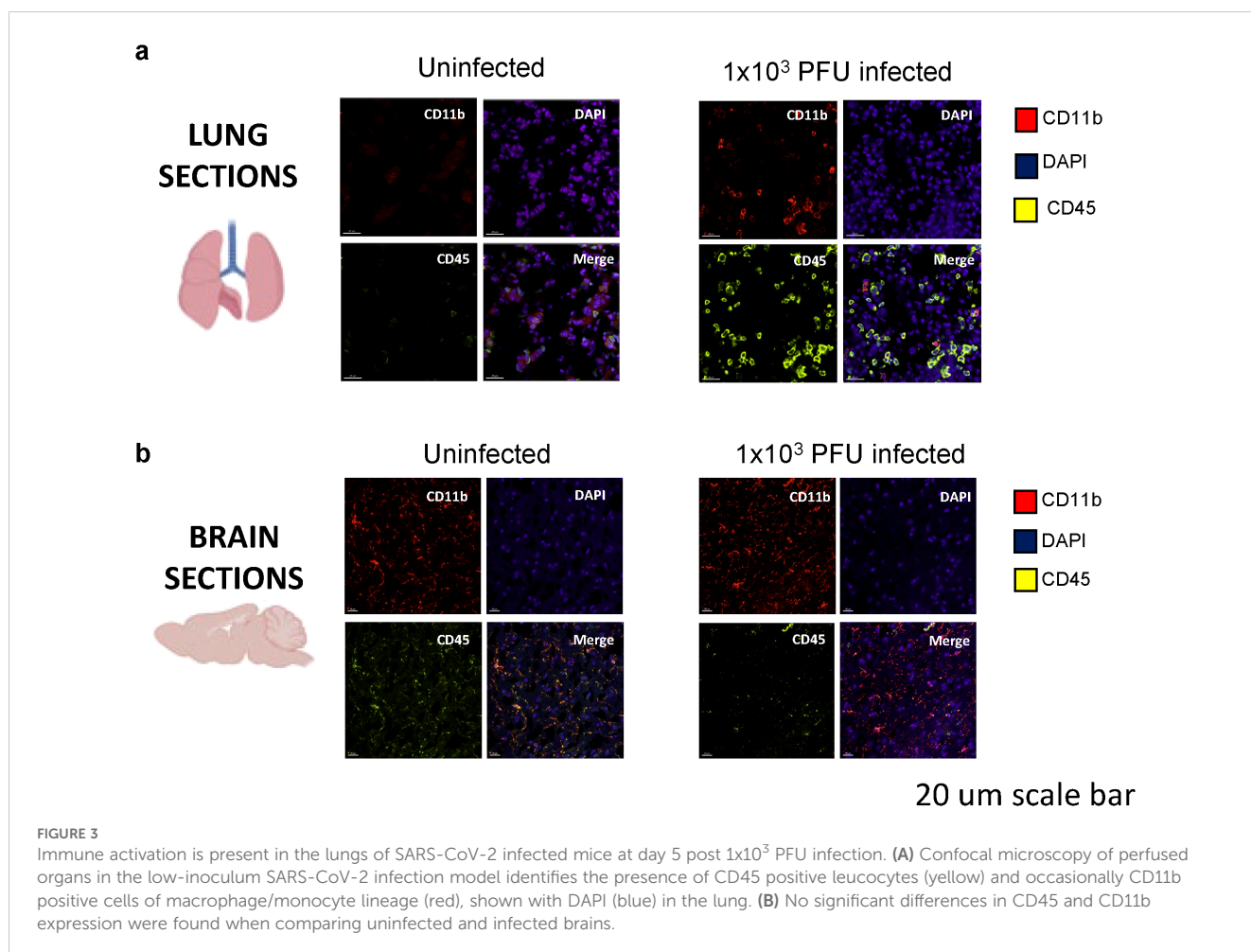
### Brains from low inoculum SARS-CoV-2 infected mice showed immune activation and increases in microglial reactivity despite the absence of active SARS-CoV-2 replication

Brains from low inoculum mice showed no detectable viral proteins (checked by spike staining) and no detectable viral transcription (checked using subgenomic E). However, these

brains showed reactive microglia, with increased Iba1 expression (as measured by percentage area, fluorescence intensity and reactivation indices, Figures 5A–F). Clusters of GFAP+ astrocytes were found in the regions of high Iba1 expression in the brain, suggesting concomitant microgliosis and astrogliosis, as has been reported in human post-mortem samples (Supplementary Figures 3A, B). To ask whether parainfectious brain injury with potential blood-brain-barrier damage had taken place, the brain supernatant/serum albumin ratios were measured in uninfected mice and low inoculum infected animals (Supplementary Figure 3C). In humans post-COVID-19, NfL has been found to be raised, but there were no significant differences in the brain injury marker NfL, either by ELISA or Simoa (Supplementary Figure 3D) at this early time point (day 5 post infection) (7).

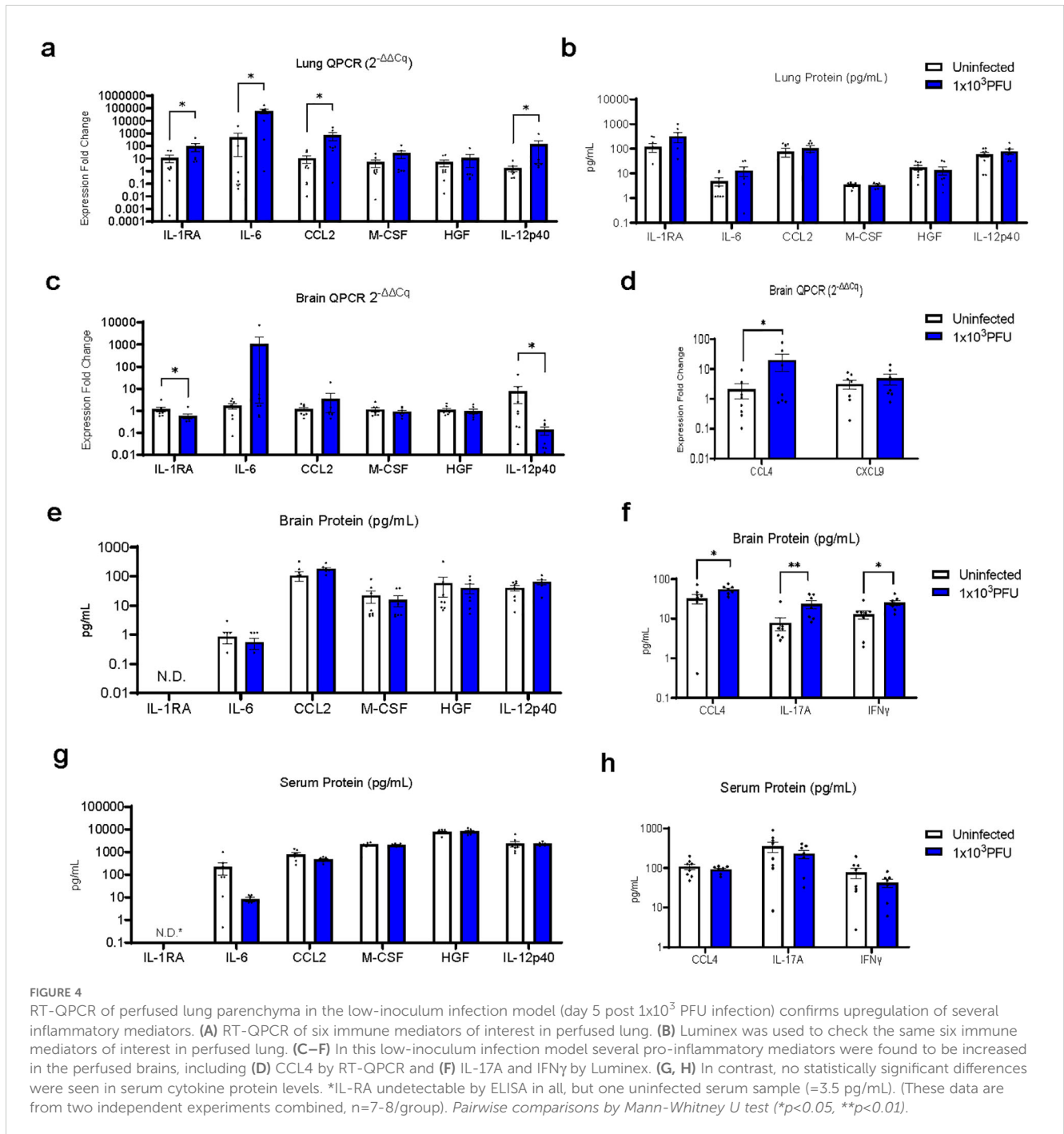
### Viral effects on endothelial cells *in vitro* lead to pro-inflammatory cytokine production and subsequent microglia reactivation

We hypothesized that the cerebral vasculature is the most common route for SARS-CoV-2 infection interacting with neuroglial cells and causing local, not necessarily systemic, inflammation. To study the cascade of events in a controlled



environment, we exposed mouse endothelial cells (bEnd.3 cell line) to inactivated SARS-CoV-2 viral particles at three multiplicities of infection (MOI), collected and filtered the supernatant, and measured the cytokines present. The TLR3 agonist polyI:C served as a positive control (Figures 6A, B). The MOIs of 0.1 and 1 used to treat endothelial cells produced significant amounts of pro-inflammatory cytokines IL-6 and CCL2, so the MOI of 1 was chosen for the subsequent experiments as a way to mirror direct infection of brain endothelial cells, but not microglia and astrocytes

(Figures 6C–E; Supplementary Figures 4A, B). Primary mouse microglia and astrocytes were exposed to the filtered supernatant from endothelial cells and their cytokine production and for microglia, their reactivation index was measured by Iba1+ morphology (Figures 6D, E; Supplementary Figures 4A, B). The supernatant from MOI=1 exposed endothelial cells resulted in the highest reactivation index indicating a pathway by which SARS-CoV-2 can indirectly affect brain cells and which is consistent with our *in vivo* data.



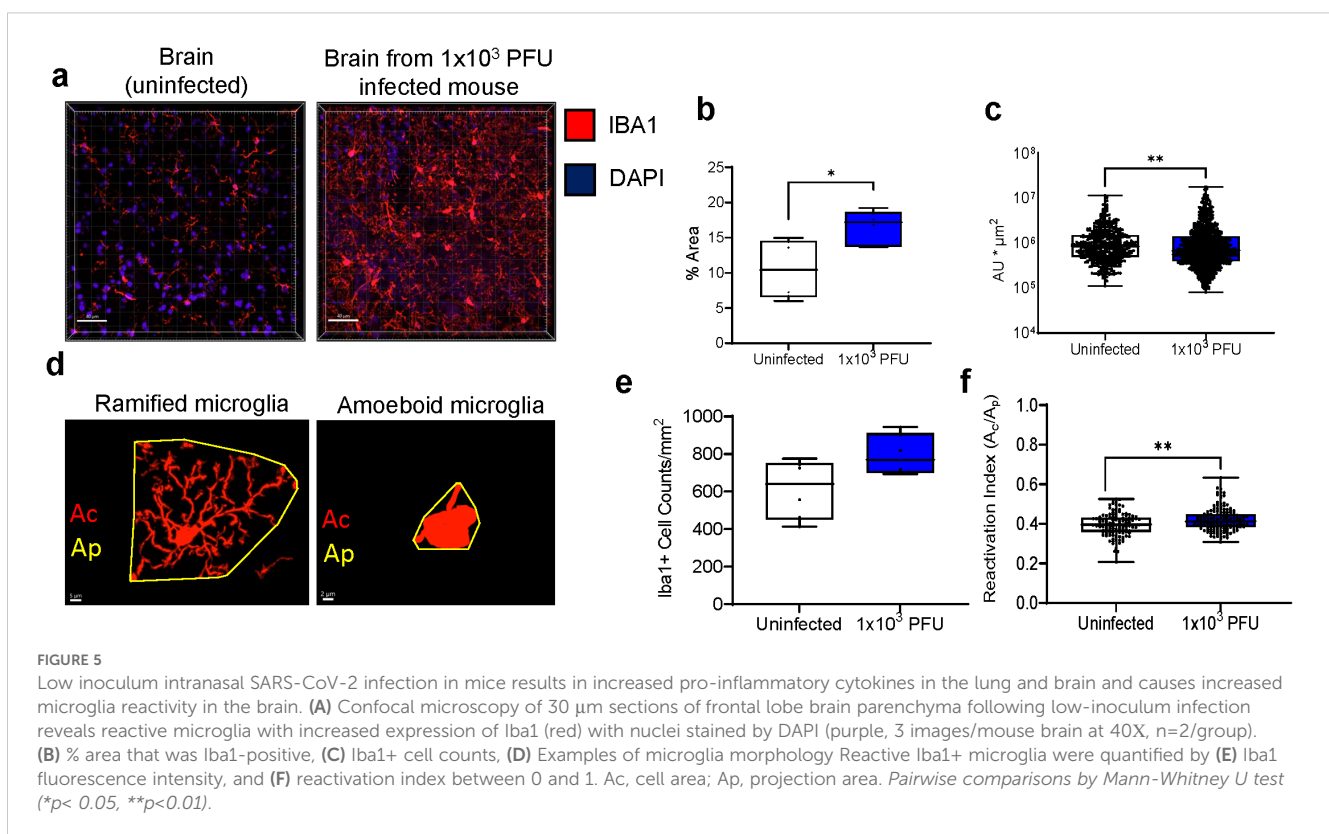
## Discussion

To better study the acute host response in SARS-CoV-2, and given that SARS-CoV-2 is rarely identified in the brain parenchyma in clinical samples, we developed a low-inoculum mouse model of COVID-19 which induced pulmonary infection in the absence of replication of virus in the brain. Following intranasal administration, by five days the mice had developed evidence of lung infection and immune cell infiltration (18), with production of inflammatory mediators, including CCL2, IL-6, IL-12p40 and IL-1RA; these cytokines were also elevated acutely in the serum of COVID-19 patients with low Glasgow coma scale scores (7). Despite the absence of viral replication in the brain parenchyma, there was some, albeit limited, production of inflammatory mediators in the brain, including CCL4, IFN $\gamma$  and IL-17A. In addition, there was an increase in microglial Iba1 staining and microglia reactivation morphology. We had expected to also see increased numbers of CD45+ and CD11b+ cells, but believe that this was limited by the thin cryosections examined. In fact, we needed to examine thicker cryosections in order to quantify the microglia morphology (17). In future studies, flow cytometry would be an important way to quantify immune cell infiltration. Immune infiltrates and microgliosis were also observed in our previous mouse studies (19, 20). Parallel *in vitro* studies demonstrated that the filtered supernatant from brain endothelial cells exposed to SARS-CoV-2 virions, induced activation of microglia and production of CCL2. Our *in vitro* model using inactivated virus (due to limitations on CL3 work) delivered viral particles to

endothelial cells and we hypothesize that this strongly stimulated them via innate PAMP pathways such as TLRs. Building on this, future studies could apply similar approaches to compare direct and indirect effects of vaccines and active virus on neuroglial cells. Active viruses would stimulate by DAMPs and PAMPs.

Our findings suggest that a primarily pulmonary inflammatory process is rapidly associated with parainfectious immune activation in the brain and the signature of an NK cell and/or T cell response which indicates a cascade of inflammation potentially amenable to treatment. Our mouse model is novel in using a low inoculum of SARS-CoV-2 virus for infection which does not induce lethal brain pathology, allowing us to study the immune activation in the brain in the absence of direct viral invasion. This is congruent with the majority of human autopsy results which show limited virus in the brain, but nevertheless demonstrate inflammation and microglia reactivity (21, 22). Human autopsy studies have studied this concept and found that exposure to lung-derived cytokines is association with microglia activation and that this was reduced by corticosteroid treatment (23). This may also reflect longer term effects, as a hamster model which examined neuropathology at 31 days post-SARS-CoV-2 infection found that Iba1 expression remained elevated (24). Studies of brain organoids have reported that Iba1+ microglia engulf post-synaptic material contributing to synapse elimination (25).

There have been reports of viral encephalitis and neuron degeneration and apoptosis observed in non-human primates (26, 27). Interestingly, in these studies the virus was present at low amounts in the brain and was found predominantly in the



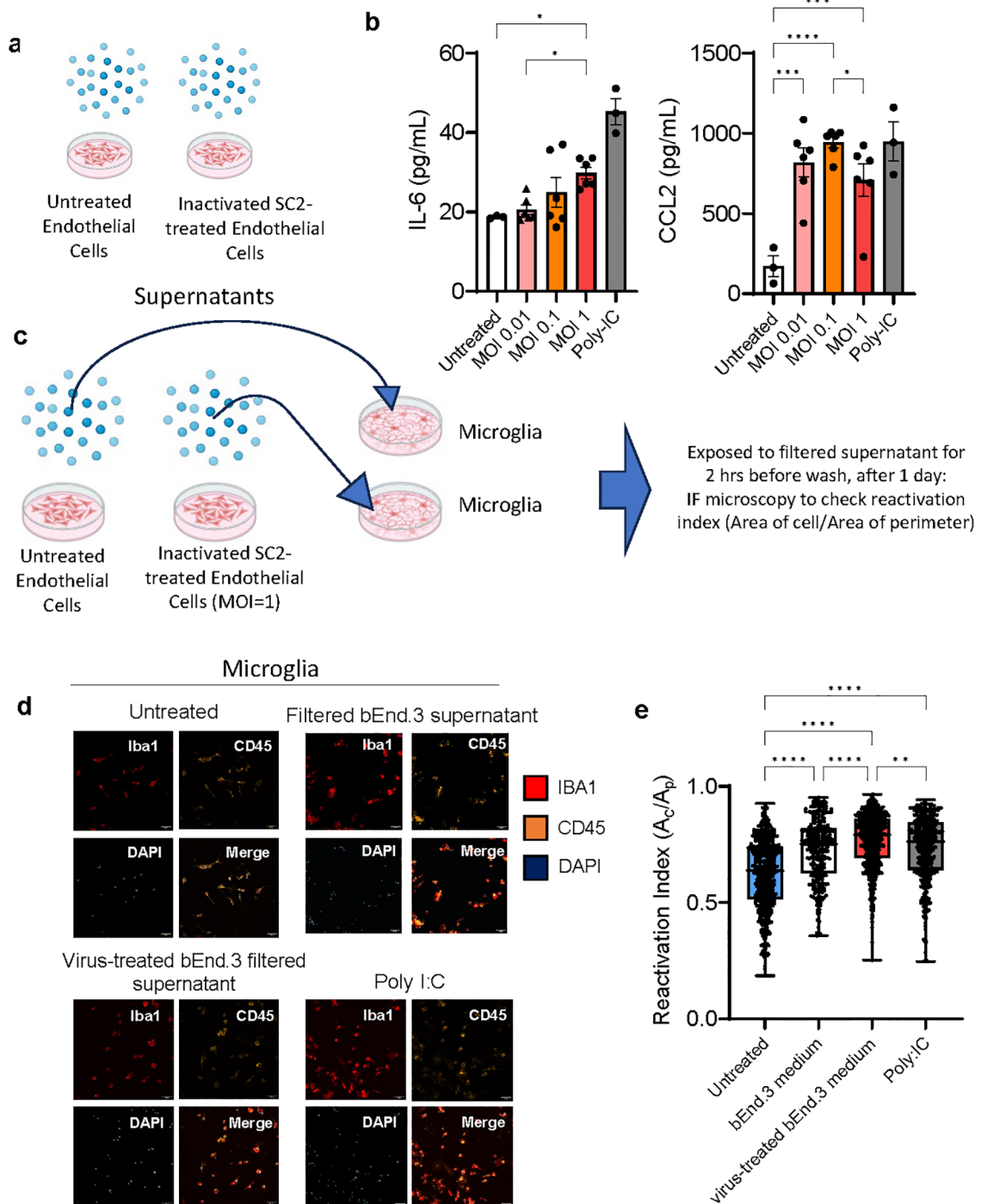


FIGURE 6

Viral effects on endothelial cells *in vitro* lead to pro-inflammatory cytokine production and subsequent microglia reactivation. (A, B) bEnd.3 cells were treated with heat and acid inactivated SARS-CoV-2 at a ratio of 0.01,0.1, or 1 virus copies per cell for 24 hours. At 24 hours concentrations of cytokines IL-6 and CCL2 were determined by ELISA and groups compared by ANOVA \* $p < 0.05$ , \*\* $p < 0.01$ , \*\*\* $p < 0.001$ , \*\*\*\* $p < 0.0001$ . (C–E) Primary mouse microglia were treated with 20 nm filtered supernatant taken from bEnd. 3 cells incubated with virus at an MOI of 1, for 2 hours, before being washed and culture medium replaced. At 24 hours cells were fixed and immunostained for Iba1 and CD45 and imaged by confocal microscopy. 6–7 separate wells were cultured for each treatment condition and 3–4 for each control condition, with 16 images taken per well at 25x magnification. Dots represent individual cells. Groups compared by Kruskal-Wallis \* $p < 0.05$ , \*\* $p < 0.01$ , \*\*\* $p < 0.001$ , \*\*\*\* $p < 0.0001$ .

vasculature as visualized by co-localization with Von Willebrand Factor (27). Mimicking the clinical scenario, there was no correlation found between neurological markers with severity of respiratory disease. Another study reported increased CCL11 (eotaxin) in mouse serum and CSF that correlated with demyelination (28). That mouse model also lacked direct viral neural invasion by infecting mice that were intratracheally transfected with human ACE2. The demyelination was also observed after intraperitoneal administration of CCL11. Interestingly, clinical studies showed higher plasma levels of CCL11 in the patients who had brain fog (28). We did not observe elevated serum cytokines in our studies and this could be due to severity, timepoint, and/or technical differences. Our negative results in the serum are at least in part contributed to by heat-inactivation of experimental samples, which were part of safety protocols in the CL3 lab at the point when these experiments were conducted (29). Hamster studies have showed that COVID-19 leads to IL-1 $\beta$  and IL-6 expression within the hippocampus and medulla oblongata and is associated with decreased neurogenesis in the hippocampal dentate gyrus which leads to learning and memory deficits (30). This has also been shown in direct *in vitro* assays—with application of serum from COVID-19 patients with delirium with elevated IL-6 leading to decreased proliferation and increased apoptosis of a human hippocampal progenitor cell line (31). Our *in vitro* studies enabled us to isolate a potential mechanism by which SARS-CoV-2 indirectly affects brain cells—by studying endothelial cells which express ACE2 and can be directly infected by the virus (15), collecting their supernatants containing pro-inflammatory cytokines, and exposing microglia and astrocytes to them. Spike protein alone has previously been found to cause inflammation and associated cognitive deficits in animal models which is a common and important long-lasting symptom of COVID-19 in humans (32–34).

In conclusion, the low inoculum SARS-CoV-2 mouse model and parallel *in vitro* studies highlight an approach to study parainfectious effects on the brain and enables characterisation of the neuroglial cells themselves. The cytokine signature and microglia reactivity post infection indicate an acute local immune response including initial inflammation in the absence of active viral replication in the brain that could be amenable to targeted immunosuppression which can direct future studies.

## Data availability statement

The raw data supporting the conclusions of this article will be made available by the authors, without undue reservation.

## Ethics statement

The animal study was approved by an AWERB-approved protocol was followed for the mouse studies (University of

Liverpool Animal Welfare and Ethical Review Body, UK Home Office Project Licence PP4715265. The study was conducted in accordance with the local legislation and institutional requirements.

## Author contributions

CD: Formal analysis, Investigation, Writing – original draft, Conceptualization, Funding acquisition, Methodology, Visualization. CH: Formal analysis, Investigation, Methodology, Visualization, Writing – review & editing. SB: Formal analysis, Writing – review & editing. JJC: Methodology, Writing – review & editing. PS: Methodology, Writing – review & editing. KS: Methodology, Writing – review & editing. KT: Formal analysis, Writing – review & editing. EN: Writing – review & editing. RW: Writing – review & editing. AF: Writing – review & editing. HF: Writing – review & editing. YH: Writing – review & editing. GW: Writing – review & editing. CC: Writing – review & editing. ME: Writing – review & editing. MH: Formal analysis, Methodology, Visualization, Writing – review & editing. FE: Writing – review & editing. MG: Writing – review & editing. TS: Writing – review & editing. GB: Writing – review & editing. AK: Writing – review & editing. JC: Writing – review & editing. SI: Writing – review & editing. AV: Conceptualization, Investigation, Visualization, Writing – original draft, Writing – review & editing. JS: Funding acquisition, Investigation, Methodology, Project administration, Resources, Writing – review & editing, Supervision. LT: Investigation, Methodology, Writing – review & editing, Supervision. DM: Writing – review & editing, Conceptualization, Investigation, Supervision, Visualization. BM: Writing – original draft, Writing – review & editing, Conceptualization, Funding acquisition, Investigation, Methodology, Project administration, Resources, Supervision, Visualization.

## Funding

The author(s) declare financial support was received for the research, authorship, and/or publication of this article. This research was funded by the National Institute for Health and Care Research (NIHR) (CO-CIN-01) and jointly by NIHR and UK Research and Innovation (CV220-169, MC\_PC\_19059). BDM is supported by the UKRI/MRC (MR/V03605X/1), the MRC/UKRI (MR/V007181/1), MRC (MR/T028750/1) and Wellcome (ISSF201902/3). BDM is also supported by the NIHR Health Protection Research Unit (HPRU) in Emerging and Zoonotic Infections at University of Liverpool in partnership with Public Health England (PHE), in collaboration with Liverpool School of Tropical Medicine and the University of Oxford [award 200907], NIHR HPRU in Respiratory Infections at Imperial College London with PHE [award 200927]. CD is supported by MRC (MC\_PC\_19044). We acknowledge the Liverpool Centre for Cell Imaging (CCI) for provision of imaging equipment (Dragonfly

confocal microscope) and excellent technical assistance (BBSRC grant number BB/R01390X/1). TS is supported by The Pandemic Institute and the NIHR Health Protection Research Unit (HPRU) in Emerging and Zoonotic Infections at University of Liverpool. DM and EN are supported by the NIHR Cambridge Biomedical Centre and by NIHR funding to the NIHR BioResource (RG94028 and RG85445), and by funding from Brain Research UK 201819-20.

## Conflict of interest

The authors declare that the research was conducted in the absence of any commercial or financial relationships that could be construed as a potential conflict of interest.

## Publisher's note

All claims expressed in this article are solely those of the authors and do not necessarily represent those of their affiliated

organizations, or those of the publisher, the editors and the reviewers. Any product that may be evaluated in this article, or claim that may be made by its manufacturer, is not guaranteed or endorsed by the publisher.

## Author disclaimer

The views expressed are those of the author(s) and not necessarily those of the UKRI, NHS, the NIHR or the Department of Health and Social Care.

## Supplementary material

The Supplementary Material for this article can be found online at: <https://www.frontiersin.org/articles/10.3389/fimmu.2024.1440324/full#supplementary-material>

## References

- Grundmann A, Wu C-H, Hardwick M, Baillie JK, Openshaw PJM, Semple MG, et al. Fewer COVID-19 neurological complications with dexamethasone and remdesivir. *Ann Neurol.* (2023) 93:1:88–102. doi: 10.1002/ana.26536
- Xu E, Xie Y, Al-Aly Z. Long-term neurologic outcomes of COVID-19. *Nat Med.* (2022), 1–10. doi: 10.1038/s41591-022-02001-z
- Meinhardt J, Radke J, Dittmayer C, Franz J, Thomas C, Mothes R, et al. Olfactory transmucosal SARS-CoV-2 invasion as a port of central nervous system entry in individuals with COVID-19. *Nat Neurosci.* (2021) 24:168–75. doi: 10.1038/s41593-020-00758-5
- Matschke J, Lütgehetmann M, Hagel C, Spherhake JP, Schröder AS, Edler C, et al. Neuropathology of patients with COVID-19 in Germany: a post-mortem case series. *Lancet Neurol.* (2020) 19:919–29. doi: 10.1016/S1474-4422(20)30308-2
- Khan M, Yoo S-J, Clijsters M, Backaert W, Vanstapel A, Speleman K, et al. Visualizing in deceased COVID-19 patients how SARS-CoV-2 attacks the respiratory and olfactory mucosae but spares the olfactory bulb. *Cell.* (2021) 184:5932–5949.e15. doi: 10.1016/j.cell.2021.10.027
- Dunai C, Collie C, Michael BD. Immune-mediated mechanisms of COVID-19 neuropathology. *Front Neurol.* (2022) 13. doi: 10.3389/fneur.2022.882905
- Michael BD, Dunai C, Needham EJ, Tharmaratnam K, Williams R, Huang Y, et al. Para-infectious brain injury in COVID-19 persists at follow-up despite attenuated cytokine and autoantibody responses. *Nat Commun.* (2023) 14:8487. doi: 10.1038/s41467-023-42320-4
- Needham EJ, Ren AL, Digby RJ, Norton EJ, Ebrahimi S, Outtrim JG, et al. Brain injury in COVID-19 is associated with dysregulated innate and adaptive immune responses. *Brain.* (2022), awac321. doi: 10.1093/brain/awac321
- Frontera JA, Sabadia S, Lalchan R, Fang T, Flusty B, Millar-Verneti P, et al. A prospective study of neurologic disorders in hospitalized patients with COVID-19 in New York City. *Neurology.* (2021) 96:e575–86. doi: 10.1212/WNL.0000000000010979
- Thwaites RS, Sanchez Sevilla Uruchurtu A, Siggins MK, Liew F, Russell CD, et al. Inflammatory profiles across the spectrum of disease reveal a distinct role for GM-CSF in severe COVID-19. *Sci Immunol.* (2021) 6:eabg9873. doi: 10.1126/sciimmunol.abg9873
- Leist SR, Dinno KH, Schäfer A, Tse LV, Okuda K, Hou YJ, et al. A mouse-adapted SARS-CoV-2 induces acute lung injury and mortality in standard laboratory mice. *Cell.* (2020) 183:1070–1085.e12. doi: 10.1016/j.cell.2020.09.050
- Carossino M, Montanaro P, O'Connell A, Kenney D, Gertje H, Grosz KA, et al. Fatal neuroinvasion and SARS-CoV-2 tropism in K18-hACE2 mice is partially independent on hACE2 expression. *Viruses.* (2021) 14(3):535. doi: 10.1101/2021.01.13.425144
- Golden JW, Cline CR, Zeng X, Garrison AR, Carey BD, Mucker EM, et al. Human angiotensin-converting enzyme 2 transgenic mice infected with SARS-CoV-2 develop severe and fatal respiratory disease. *JCI Insight.* (2020) 5. doi: 10.1172/jci.insight.142032
- Kumari P, Rothan HA, Natekar JP, Stone S, Pathak H, Strate PG, et al. Neuroinvasion and encephalitis following intranasal inoculation of SARS-CoV-2 in K18-hACE2 mice. *Viruses.* (2021) 13:132. doi: 10.3390/v13010132
- Wenzel J, Lampe J, Müller-Fielitz H, Schuster R, Zille M, Müller K, et al. The SARS-CoV-2 main protease Mpro causes microvascular brain pathology by cleaving NEMO in brain endothelial cells. *Nat Neurosci.* (2021) 24:1522–33. doi: 10.1038/s41593-021-00926-1
- Wittekindt M, Kaddatz H, Joost S, Staffeld A, Bitar Y, Kipp M, et al. Different methods for evaluating microglial activation using anti-ionized calcium-binding adaptor protein-1 immunohistochemistry in the cuprizone model. *Cells.* (2022) 11:1723. doi: 10.3390/cells11111723
- Heindl S, Gesierich B, Benakis C, Llovera G, Duering M, Liesz A. Automated morphological analysis of microglia after stroke. *Front Cell Neurosci.* (2018) 12. doi: 10.3389/fncel.2018.00106
- Santos Bravo M, Berengua C, Marín P, Esteban M, Rodriguez C, del Cuerpo M, et al. Viral culture confirmed SARS-CoV-2 subgenomic RNA value as a good surrogate marker of infectivity. *J Clin Microbiol.* (2022) 60:e01609–21. doi: 10.1128/JCM.01609-21
- De Neck S, Penrice-Randal R, Clark JJ, Sharma P, Bentley EG, Kirby A, et al. The stereotypic response of the pulmonary vasculature to respiratory viral infections: findings in mouse models of SARS-CoV-2, influenza A and gammaherpesvirus infections. *Viruses.* (2023) 15:1637. doi: 10.3390/v15081637
- Seehusen F, Clark JJ, Sharma P, Subramaniam K, Giuliani SW, Hughes GL, et al. Viral Neuroinvasion and Neurotropism without Neuronal Damage in the hACE2 Mouse Model of COVID-19. *Viruses.* (2021) 14(5):1020. doi: 10.1101/2021.04.16.440173
- Thakur KT, Miller EH, Glendinning MD, Al-Dalahmah O, Banu MA, Boehme AK, et al. COVID-19 neuropathology at Columbia University Irving Medical Center/ New York Presbyterian Hospital. *Brain.* (2021) 144:2696–708. doi: 10.1093/brain/awab148
- Lee MH, Perl DP, Steiner J, Pasternack N, Li W, Maric D, et al. Neurovascular injury with complement activation and inflammation in COVID-19. *Brain J Neurol.* (2022) 145:2555–68. doi: 10.1093/brain/awac151
- Grant RA, Poor TA, Sichizya L, Diaz E, Bailey JI, Soni S, et al. Prolonged exposure to lung-derived cytokines is associated with activation of microglia in patients with COVID-19. *JCI Insight.* (2024) 9:e178859. doi: 10.1172/jci.insight.178859
- Frere JJ, Serafini RA, Pryce KD, Zazhytska M, Oishi K, Golyner I, et al. SARS-CoV-2 infection in hamsters and humans results in lasting and unique systemic perturbations after recovery. *Sci Transl Med.* (2022) 14:eabq3059. doi: 10.1126/scitranslmed.abq3059
- Samudiyata, Oliveira AO, Malwade S, Rufino de Sousa N, Goparaju SK, Gracias J, et al. SARS-CoV-2 promotes microglial synapse elimination in human brain organoids. *Mol Psychiatry.* (2022) 27:3939–50. doi: 10.1038/s41380-022-01786-2

26. Choudhary S, Kanevsky I, Yildiz S, Sellers RS, Swanson KA, Franks T, et al. Modeling SARS-CoV-2: comparative pathology in rhesus macaque and golden Syrian hamster models. *Toxicol Pathol.* (2022) 50(3):280–93. doi: 10.1177/01926233211072767
27. Rutkai I, Mayer MG, Hellmers LM, Ning B, Huang Z, Monjure CJ, et al. Neuropathology and virus in brain of SARS-CoV-2 infected non-human primates. *Nat Commun.* (2022) 13:1745. doi: 10.1038/s41467-022-29440-z
28. Fernández-Castañeda A, Lu P, Geraghty AC, Song E, Lee M-H, Wood J, et al. Mild respiratory COVID can cause multi-lineage neural cell and myelin dysregulation. *Cell.* (2022) 185:2452–2468.e16. doi: 10.1016/j.cell.2022.06.008
29. Xu E, Li T, Chen Q, Wang Z, Xu Y. Study on the effect and application value of heat-inactivated serum on the detection of thyroid function, tumor markers, and cytokines during the SARS-CoV-2 pandemic. *Front Med.* (2021) 8. doi: 10.3389/fmed.2021.742067
30. Soung AL, Vanderheiden A, Nordvig AS, Sissoko CA, Canoll P, Mariani MB, et al. COVID-19 induces CNS cytokine expression and loss of hippocampal neurogenesis. *Brain.* (2022), awac270. doi: 10.1093/brain/awac270
31. Borsini A, Merrick B, Edgeworth J, Mandal G, Srivastava DP, Vernon AC, et al. Neurogenesis is disrupted in human hippocampal progenitor cells upon exposure to serum samples from hospitalized COVID-19 patients with neurological symptoms. *Mol Psychiatry.* (2022), 1–13. doi: 10.1038/s41380-022-01741-1
32. Fontes-Dantas FL, Fernandes GG, Gutman EG, De Lima EV, Antonio LS, Hammerle MB, et al. SARS-CoV-2 Spike protein induces TLR4-mediated long-term cognitive dysfunction recapitulating post-COVID-19 syndrome in mice. *Cell Rep.* (2023) 42:112189. doi: 10.1016/j.celrep.2023.112189
33. Oh J, Cho W-H, Barcelon E, Kim KH, Hong J, Lee SJ. SARS-CoV-2 spike protein induces cognitive deficit and anxiety-like behavior in mouse via non-cell autonomous hippocampal neuronal death. *Sci Rep.* (2022) 12:5496. doi: 10.1038/s41598-022-09410-7
34. Wood GK, Sargent BF, Ahmad ZUA, Tharmaratnam K, Dunai C, Egbe FN. Post-hospitalisation COVID-19 cognitive deficits at one year are global and associated with elevated brain injury markers and grey matter volume reduction. *Nat Med.* (2024), 1–1.

## COPYRIGHT

© 2024 Dunai, Hetherington, Boardman, Clark, Sharma, Subramaniam, Tharmaratnam, Needham, Williams, Huang, Wood, Collie, Fower, Fox, Ellul, Held, Egbe, Griffiths, Solomon, Breen, Kipar, Cavanagh, Irani, Vincent, Stewart, Taams, Menon and Michael. This is an open-access article distributed under the terms of the [Creative Commons Attribution License \(CC BY\)](https://creativecommons.org/licenses/by/4.0/). The use, distribution or reproduction in other forums is permitted, provided the original author(s) and the copyright owner(s) are credited and that the original publication in this journal is cited, in accordance with accepted academic practice. No use, distribution or reproduction is permitted which does not comply with these terms.